Ozonation of Single-Walled Carbon Nanotubes and Their Assemblies on Rigid Self-Assembled Monolayers

Lintao Cai, Jeffrey L. Bahr, Yuxing Yao, and James M. Tour*

Department of Chemistry and Center for Nanoscale Science and Technology, MS 222, Rice University, 6100 Main Street, Houston, Texas 77005

Received March 15, 2002. Revised Manuscript Received July 1, 2002

Ozonation of single-walled carbon nanotubes (O_3-SWNTs) produces oxygenated functional groups, e.g., carboxylic acid, ester, and quinone moieties, which can be removed from the SWNT surface by heating at 600−800 °C. The annealed SWNTs appear to be pristine. The electrical resistance of the O_3-SWNTs depends on the degree of oxidation and is about 20−2000 times higher than that of pristine SWNTs, owing to the deformation of the π-conjugation structure along the tube. The O_3-SWNTs are easily dispersed in dimethylformamide (DMF) and show enhanced solubility in other polar solvents such as water and ethanol. The O_3-SWNT suspensions consist of individual and shortened tubes due to the separation of nanotube bundles and the shortening that results from oxidation. Toward fabrication of SWNT-based molecular electronic devices, two methods have been used to assemble the O_3-SWNTs on functionalized self-assembled monolayers (SAMs) of conjugated oligo(phenylene ethynylene)s. The first, termed "chemical assembly", is based on a condensation reaction between the carboxylic acid functionalities of O_3-SWNTs and the amine functionalities of SAMs to form amides. The results show that O_3-SWNTs coat the amino-terminated SAM with a high degree of surface coverage. The second method is based on physical adsorption via layer-by-layer (LBL) deposition with bridging of metal cations, i.e., Fe^{3+} on carboxylate-terminated SAMs or Cu^{2+} on thiol-terminated SAMs. The oxidatively shortened O_3-SWNTs are shown to be perpendicular to the surface with random adsorption of longer tubes. The patterned nanotube assemblies may be useful in hybridized electronic devices, where device functions can be modified by the orientation and stacking of SWNTs and the properties of the SAM.

Introduction

Single-walled carbon nanotubes[1] (SWNTs) have been intensively investigated due to their unique one-dimensional structure with adjustable electronic conductivity and robust mechanical properties. Possible applications[2−4] include nanoelectronics, flat-panel display devices, energy storage, and space technology. Much work has been done on the controlled functionalization at the ends or sidewalls of SWNTs by chemical modification or physical adsorption. Indeed, SWNTs have been functionalized via electrochemical or thermal reduction of aryl diazonium salts,[5] by reaction with fluorine[6,7] and subsequent alkylation,[8] and by noncovalent adsorption for protein immobilization.[9] SWNTs have also been used as tips for high resolution, chemically sensitive images and nanolithography.[10,11] Ozonation of amorphous carbon leads to the production of surface hydroxyl, carbonyl, and carboxylic acid functional groups.[12] A fullerene ozonide has been formed by ozonation of C_{60} to a $C_{60}O$ structure in hydrocarbon solution.[13] The reaction of O_3 with SWNTs has also been reported,[14] resulting in end etching and production of surface functional groups such as esters and quinones.

* Corresponding author. Fax: 713-348-6250. E-mail: tour@rice.edu.

(1) Dekker: C. *Phys. Today* **1999**, *52*, 22.

(2) (a) Fan, S.; Chapline, M. G.; Franklin, N. R.; Tombler, T. W.; Cassell, A. M.; Dai, H. *Science* **1999**, *283*, 512. (b) Collins, P.; Bradley, K.; Ishigami, M.; Zettl, A. *Science* **2000**, *287*, 1801.

(3) Jhi, S.-H.; Louie, S. G.; Cohen, M. L. *Phys. Rev. Lett.* **2000**, *85*, 1710.

(4) (a) Dillon, A. C.; Jones, K. M.; Bekkedal, T. A.; Kiang, C. H.; Bethume, D. S.; Heben, M. J. *Nature* **1997**, *386*, 377. (b) Che, G. L.; Lakshmi, B. B.; Fisher, E. R.; Martin, C. R. *Nature* **1998**, *393*, 346.

(5) (a) Bahr, J. L.; Yang, J.; Kosynkin, D. V.; Bronikowski, M. J.; Smalley, R. E.; Tour, J. M. *J. Am. Chem. Soc.* **2001**, *123*, 6536. (b) Bahr, J. L.; Tour, J. M. *Chem. Mater.* **2001**, *13*, 3823.

(6) Mickelson, E. T.; Huffman, C. B.; Rinzler, A. G.; Smalley, R. E.; Hauge, R. H.; Margrave.J. L. *Chem. Phys. Lett.* **1998**, *296*, 188.

(7) Mickelson, E. T.; Chiang, I. W.; Zimmerman, J. L.; Boul, P. J.; Lozano, J.; Liu, J.; Smalley, R. E.; Hauge, R. H.; Margrave.J. L. *J. Phys. Chem. B*, **1999**, *103*, 4318.

(8) Boul, P.; Liu, J.; Mickelson, E.; Huffman, C.; Ericson, L.; Chiang, I.; Smith, K.; Colbert, D.; Hauge, R.; Margrave, J.; Smalley, R. E. *Chem. Phys. Lett.* **1999**, *310*, 367.

(9) Chen, R. J.; Zhang, Y.; Wang, D.; Dai, H. *J. Am. Chem. Soc.* **2001**, *123*, 3838.

(10) (a) Wong, S. S.; Joselevich, E.; Woolley, A. T.; Cheung, C. L.; Lieber, C. M. *Nature* **1998**, *394*, 52. (b) Wong, S. S.; Woolley, A. T.; Joselevich, E.; Cheung, C. L.; Lieber, C. M. *J. Am. Chem. Soc.* **1998**, *120*, 8557.

(11) Cheung, C. L.; Hafner, J. H.; Lieber, C. M. *Proc. Natl. Acad. Sci. U.S.A.* **2000**, *97*, 3809.

(12) Mawhinney, D. B.; Yates, J. T., Jr. *Carbon* **2001**, *39*, 1167.

(13) (a)Weisman, R. B.; Heymann, D.; Bachilo, S. M.*J. Am. Chem. Soc.* **2001**, *123*, 9720. (b) Heymann, D.; Bachilo, S. M.; Weisman, R. B.; Cataldo, F.; Fokkens, R. H.; Nibbering, N. M. M.; Vis, R. D.; Chibante, L. P. F. *J. Am. Chem. Soc.* **2000**, *122*, 11473.

(14) (a) Mawhinney, D. B.; Naumenko, V.; Kuznetsova, A.; Yates, J. T., Jr.; Liu, J.; Smalley, R. E. *J. Am. Chem. Soc.* **2000**, *122*, 2383. (b) Kuznetsova, A.; Mawhinney, D. B.; Naumenko, V.; Yates, J. T., Jr.; Liu, J.; Smalley, R. E. *Chem. Phys. Lett.* **2000**, *321*, 292. (c) Mawhinney, D. B.; Naumenko, V.; Kuznetsova, A.; Yates, J. T., Jr.; Liu, J.; Smalley, R. E. *Chem. Phys. Lett.* **2000**, *324*, 213. (d) Deng, J. P.; Mou, C. Y.; Han, C. C. *Fullerene Sci. Technol.* **1997**, *5*, 1033.

10.1021/cm020273o CCC: $22.00
Published on Web 09/05/2002

Etching SWNTs in an oxidizing acid mixture produces carboxylic acid groups at the open end of nanotubes; the resulting material is more soluble in water and ethanol than pristine SWNTs.[15,16] The oxidized SWNTs form perpendicularly aligned structures on metal-ion modified surfaces[17] and show a strong affinity for amine-modified substrates.[18] These SWNT-containing structures were constructed at an insulating molecular layer such as polyions, alkanethiols, and silanizing reagents. For the fabrication of SWNT-based molecular electronic devices, conjugated organic molecules with π-orbital overlap are required for charge transport and functional devices. Rigid-rod conjugated oligo(phenylene ethynylene)s are one family of molecules that have interesting properties, such as negative differential resistance (NDR) and memory.[19]

We here report the oxidation of SWNTs in a UV/O_3 gas−solid interface reaction, and the subsequent assembly of these oxidized SWNTs on oligo(phenylene ethynylene) self-assembled monolayers (SAMs). The ozonated SWNTs (O_3-SWNTs) have been characterized by a series of analysis techniques including UV−vis, Raman, FTIR, TGA, and AFM. The O_3-SWNTs have a substantial amount of oxidized functional groups, enabling their assembly on differently functionalized SAMs (Scheme 1).

Experimental Section

Chemicals. Tetrahydrofuran (THF) was purified by distillation from sodium/benzophenone ketyl. Methylene chloride was distilled from calcium hydride. All other chemicals were used as received without further purification. The SWNTs were obtained from the gas-phase decomposition of CO (HiPco process).[20] SWNT purification methods[5a,21]were reported elsewhere. The average diameter of the HiPco tubes was about 0.7−0.8 nm. The syntheses of the oligo(phenylene ethynylene)s compounds have been described elsewhere.[22]

Ozonation of SWNT in UV/O_3 Gas Phase. A ca. 2 mg portion of purified SWNTs was sonicated for 1 h in 20 mL of DMF, filtered over a 0.2 μm PTFE membrane, and then dried at 150 °C for 1 h. The "bucky paper" of SWNTs thus formed was then placed in a UV/O_3 generator in ambient laboratory air for 3 h (Boekel Industries, Inc., Model 135500; the same type of UV/O_3 generator used to clean silicon wafer surfaces during semiconductor device fabrication). No attempt was made to carry out the ozonations in a dry atmosphere; it is assumed that atmospheric moisture in the presence of UV radiation converted intermediate ozonides to carboxylic acids and other functionalities (vide infra). This method of ozonation is operationally simpler than Mawhinney et al.'s use of 97:3 O_3:O_2 (70% O_3 by the time it arrived in the reaction chamber) in an IR cell[14a] and involves no additional hydrolysis step or solvent.

Self-Assembled Monolayers on Au. According to previously developed protocols for assemblies,[23] amino-terminated SAM-**1** was prepared by base-deprotection using NH_4OH with precursor **1** in acetone/MeOH (v/v = 2:1) with an assembly time of 20 h. Carboxyl-terminated SAM-**2** was prepared by acid-deprotection using H_2SO_4 (98%) with precursor **2** in CH_2Cl_2/MeOH (v/v = 2:1) with an assembly time of 20 h. Thiol-terminated SAM-**3** was prepared by acid-deprotection using H_2SO_4 (98%) with precursor **3** in CH_2Cl_2/MeOH (v/v = 2:1) with an assembly time of 1 h. The assembly processes were carried

Scheme 1. Oligo(phenylene ethynylene) SAMs and Subsequent O_3-SWNT Assemblies[a]

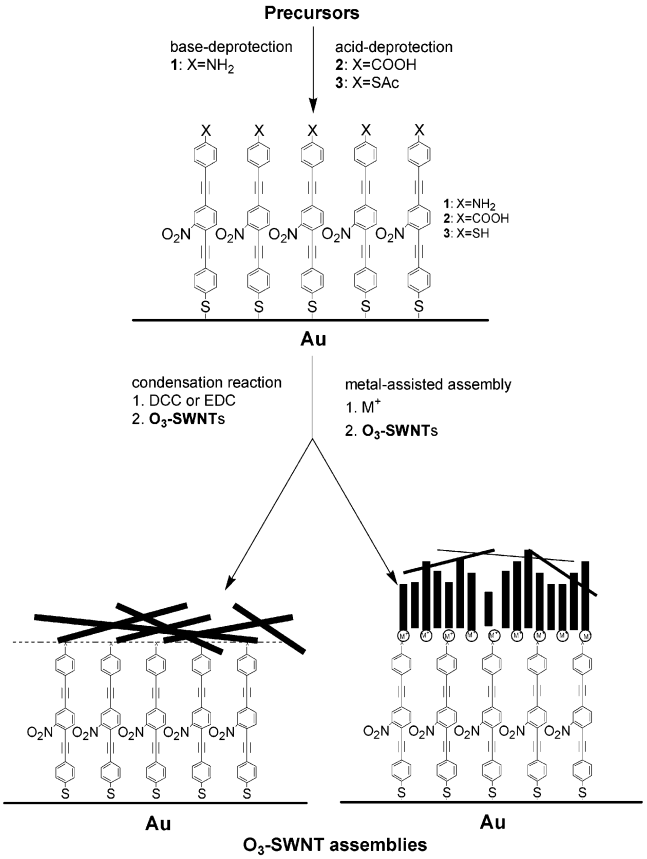

[a] The depiction is not to scale; the O_3-SWNTs are in reality much longer than the oligomers. Note that when X = SH, the nitro group could be pointing toward the gold surface or away from the gold surface.

(15) (a) Liu, J.; Rinzler, A. G.; Dai, H.; Hafner, J. H.; Bradley, R. K.; Boul, P. J.; Lu, A.; Iverson, T.; Shelimov, K.; Huffman, C. B.; R-Macias, F.; Sho, Y. S.; Lee, T. R.; Colbert, D. T.; Smalley, R. E. *Science* **1998**, *280*, 1253. (b) Chen, J.; Hamon, M. A.; Hu, H.; Chen, Y.; Rao, A. M.; Eklund, P. C.; Haddon, R. C. *Science* **1998**, *282*, 95.

(16) (a) Star, A.; Stoddart, J. F.; Steuerman, D.; Diehl, M.; Boukai, A.; Wong, E. W.; Yang, X.; Chung, S. W.; Choi, H.; Heath, J. R. *Angew. Chem., Int. Ed.* **2001**, *40*, 1721. (b) Sun, Y. P.; Huang, W. J.; Lin, Y.; Fu, K. F.; Kitaygorodskiy, A.; Riddle, L. A.; Yu, Y. J.; Carroll, D. L. *Chem. Mater.* **2001**, *13*, 2864.

(17) (a) Chattopadhyay, D.; Galeska, I.; Papadimitrakopoulos, F. *J. Am. Chem. Soc.* **2001**, *123*, 9451. (b) Wu, B.; Zhang, J.; Zhong, W.; Cai, S.; Liu, Z. *J. Phys. Chem. B* **2001,** *105*, 5075. (c) Yu, X.; Mu, T.; Huang, H.; Liu, Z.; Wu, N. *Surf. Sci.* **2000**, *461*, 199.

(18) (a)Liu, J.; Casavant, M. J.; Cox, M.; Walters, D. A.; Boul, P.; Lu, W.; Rimberg, A. J.; Smith, K. A.; Colbert, D. T.; Smalley, R. E. *Chem. Phys. Lett.* **1999**, *303*, 125. (b) Burghard, M.; Duesberg, G.; Philipp, G.; Muster, J.; Roth, S. *Adv. Mater.* **1998**, *10*, 584. (c) Liu, Z.; Shen, Z.; Zhu, T.; Hou, S.; Ying, L.; Shi, Z.; Gu, Z. *Langmuir* **2000**, *16*, 3569. (d) Nan, X.; Gu, Z.; Liu, Z. *J. Colloid. Interface Sci.* **2002**, *245*, 311.

(19) (a) Tour, J. M. *Acc. Chem. Res.* **2000**, *33*, 791. (b) Reed, M. A.; Tour, J. M. *Sci. Am.* **2000**, *282*, 68. (c) Allara, D. L.; Dunbar, T. D.; Weiss, P. S.; Bumm, L. A.; Cygan, M. T.; Tour, J. M.; Reinerth, W. A.; Yao, Y.; Kozaki, M.; Jones, II, L. *Ann. N. Y. Acad. Sci.* **1998,** *852*, 349. (d) Reed, M. A.; Chen, J.; Rawlett, A. M.; Price, D. W.; Tour, J. M. *App. Phys. Lett.* **2001**, *78*, 3735.

(20) Nikolaev, P.; Bronikowski, M. J.; Bradley, R. K.; Rohmund, F.; Colbert, D. T.; Smith, K. A.; Smalley, R. E. *Chem. Phys. Lett.* **1999**, *313*, 91.

(21) Chiang, I. W.; Brinson, B. E.; Huang, A. Y.; Willis, P. A.; Bronikowski, M. J.; Margrave, J. L.; Smalley, R. E.; Hauge, R. H. *J. Phys. Chem.* **2001**, *105*, 8297.

(22) (a) Tour, J. M.; Rawlett, A. M.; Kozaki, M.; Yao, Y.; Jagessar, R. C.; Dirk, S. M.; Price, D. W.; Reed, M. A.; Zhou, C. W.; Chen, J.; Wang, W.; Campbell, I. *Chem. Eur. J.* **2001**, *7*, 5118. (b) Tour, J. M.; Kozaki, M.; Seminario, J. M. *J. Am. Chem. Soc.* **1998**, *120*, 8486. (c) Tour, J. M.; Jones, L., II.; Pearson, D. L.; Lamba, J. S.; Burgin, T. P.; Whitesides, G. W.; Allara, D. L.; Parikh, A. N.; Atre, S. V. *J. Am. Chem. Soc.* **1995**, *117*, 9529.

(23) Cai, L.; Yao, Y.; Yang, J.; Price, D. W.; Tour, J. M. *Chem. Mater.* **2002**, *14*, 2905.

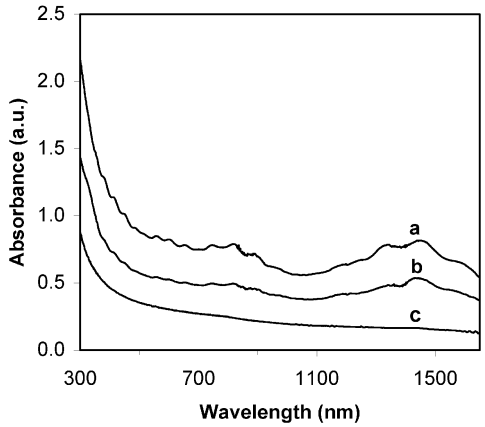

Figure 1. UV−vis spectra in dimethylformamide: (a) P-SWNT, (b) O_3-SWNT after TGA annealing in 800 °C at argon for 2 h, (c) O_3-SWNT treated with UV/O_3 for 3 h.

out in the dark under an inert atmosphere. When analyzed by ellipsometry, all of the SAMs had a film thickness that corresponded to the calculated thickness of a monolayer for each compound **1**−**3**. The molecular length is about 2.2 nm.

Assemblies of O_3-SWNTs on SAMs/Au. *(1) O_3-SWNT/SAM-***1***/Au*. SAM-**1**/Au was pretreated with 1 mM HCl for 5 min and then incubated in a 40 mg/L O_3-SWNT dispersion (pH 5) at 50 °C for 18 h, followed by addition of 400 mg/L dicyclohexyl carbodiimide (DCC, excess) for the DMF solution or 400 mg/L 1-ethyl-3-(3-dimethylaminopropyl)carbodiimide (EDC, excess) for the H_2O solution. After the modification, the sample was removed from the solution, rinsed with DMF or H_2O, acetone, and MeOH, and blown dry with N_2.

*(2) O_3-SWNT/Fe^{3+}/SAM-***2***/Au*. SAM-**2**/Au was pretreated with 1 mM NaOH for 5 min, followed by immersion in 10 mM $FeCl_3/H_2O$ (pH 2) for 15 min and then rinsing with a 1 mM NaOH/DMF solution. The samples were then incubated in 40 mg/L O_3-SWNT/DMF (pH 8.5) dispersions for 20 h. Finally, the samples were rinsed with DMF, acetone, and MeOH and blown dry with N_2.

*(3) O_3-SWNT/Cu^{2+}/SAM-***3***/Au*. SAM-**3**/Au was immersed in 10 mM $CuSO_4/H_2O$ for 15 min, rinsed with H_2O, and then incubated in 40 mg/L O_3-SWNT dispersion (pH 8.5) in DMF or H_2O solution for 20 h. The sample was rinsed with DMF/H_2O, acetone, and MeOH and blown dry with N_2.

Ellipsometry. SAM thicknesses were determined using a Rudolph series 431A ellipsometer with He−Ne laser light (632.8 nm) at 70° incident angle. The thickness was calculated on the basis of a refractive index of 1.55.[22c] The length of the conjugated oligomer was calculated from the sulfur atom to the most distant proton for the minimum energy extended forms by molecular mechanics. A bond length of 0.24 nm for the Au−S bond was used for calculating the thickness of the SAMs.

Characterization. UV−vis absorption spectra were recorded in double-beam mode with a UV/vis/NIR scanning spectrophotometer (Shimadzu, UV-3101 PC). Raman spectra were obtained with an excitation wavelength of 782 nm with a Renishaw micro-Raman spectrometer. FT-IR spectra were collected using an attenuated total reflectance (ATR) accessory. Thermogravimetric analysis (TGA) was carried out in argon. The atomic force microscopy (AFM) images were obtained in tapping mode (Nanoscope IIIa, Digital Instrument).

Results and Discussion

The small-diameter HiPco SWNTs have increased curvature strain, which leads to an enhanced reactivity compared to larger diameter SWNTs produced by other methods. All of the work described in this paper was done using HiPco SWNTs. Figure 1 shows the UV/vis/NIR absorption spectra of pristine SWNTs (P-SWNT) and ozonated SWNTs (O_3-SWNT). Ozone oxidation results in the loss of specific features present in the spectrum of P-SWNT and produces a smooth line for O_3-SWNT. This phenomenon is also observed in other functionalized SWNT.[5,7] The electronic absorption spectra of SWNTs are consistent with the local density of states and diameters of the nanotubes. The features seen in the spectrum of P-SWNT, referred to as van Hove singularities, are due to the one-dimensional nature of the energy bands. The peaks centered at 1400 and 800 nm are respectively attributed to the first and second van Hove singularity in semiconducting nanotubes, while the peaks centered around 500 nm are assigned to the first van Hove transition of metallic SWNTs. The precise position of these features is related to the diameter of the SWNT. Smaller diameter tubes exhibit shorter wavelength transitions. The width of the van Hove peaks is determined by overlapping transitions from all different diameters and chiral indices. The van Hove features are completely absent for O_3-SWNT. This indicates a significant distortion of extended π-electronic structure, presumably due to the oxidized groups. The spectra indicate that O_3-SWNT is covalently functionalized rather than a simple physical adsorption of O_3.

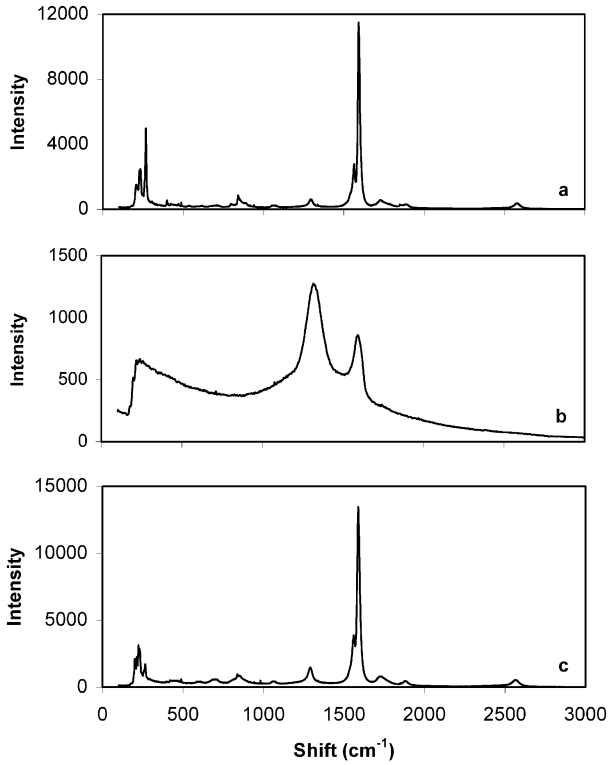

Figure 2. Raman spectra for (a) P-SWNT, (b) O_3-SWNT, and (c) O_3-SWNT after TGA.

Raman spectroscopy[24] is a powerful tool for the characterization of structure changes in SWNTs. As shown in Figure 2, the Raman spectrum of P-SWNT exhibits two strong peaks at 1590 cm^{-1} (tangential mode, ω_t) and 267 cm^{-1} (radial breathing mode, ω_r). The distribution of nanotube diameters causes the multiple peaks in the radial breathing mode region. A weak peak located at ca. 1290 cm^{-1} is assigned to the disorder

(24) Richter, E.; Subbaswamy, K. R. *Phys. Rev. Lett.* **1997**, *79*, 2738.

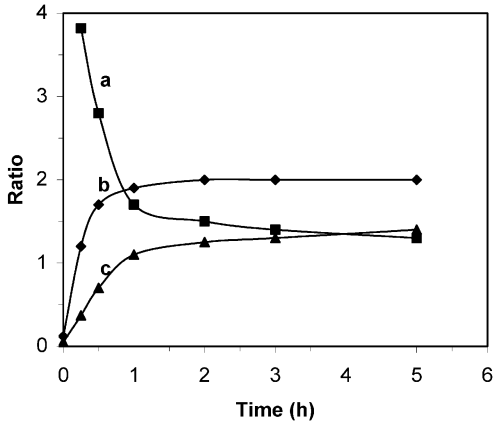

Figure 3. The relationship between Raman peak ratio of O_3-SWNT and the ozonation time: (a) ω_t/ω_r, (b) ω_d/ω_r, and (c) ω_d/ω_t.

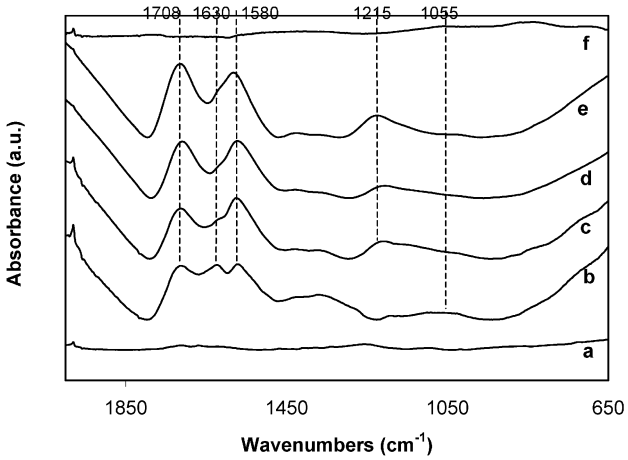

Figure 4. ATR-FT-IR spectra for (a) P-SWNT, O_3-SWNT at the different reaction times in ozone [(b) 0.5 h, (c) 1 h, (d) 3 h, (e) 5 h] and (f) O_3-SWNT after TGA. Absorbances of the major peaks ranged from less than 0.02 for P-SWNT to 0.3−0.5 for the samples taken at 3 and 5 h. The plots are stacked for illustrative purposes only; the absorbance scales are not the same for each spectrum.

structure (ω_d) which likely includes the sp^3-hybridized carbons. After the ozonation, O_3-SWNT shows a quite different character. Most notably, the relative intensity of the disorder mode is greater than that of the tangential mode. Also, the radial breathing mode is substantially broadened near 240 cm^{-1} and feature resolution is lost. On the basis of these spectroscopic changes, ozonation produces a large number of surface functional groups and increases the number of the sp^3 carbons in the SWNTs. Qualitatively speaking, the relative ratio of ω_d/ω_t and ω_d/ω_r indicates the degree of oxidation. Figure 3 illustrates the dependence of Raman peak ratios on the reaction time, i.e., the oxidation kinetics. On the basis of these data, the initial oxidation is rapid, but the reaction slows after 1 h and stops completely after 3 h, presumably due to exhaustion of active surface sites.

To differentiate the functional groups, infrared spectroscopy (ATR-FT-IR) was performed on O_3-SWNT at different reaction times. As shown in Figure 4, P-SWNTs display few features in the ATR-IR due to the very low absorbances (ca. 0.02 and below) of the complete π-electron backbone of symmetric carbons.[14a] After generation of surface-oxidized species with ozone,

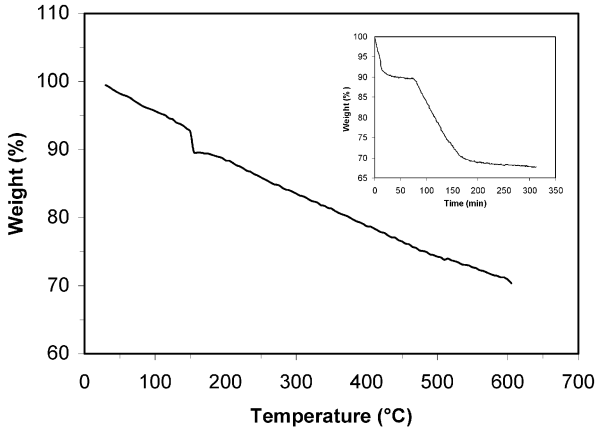

Figure 5. Thermogravimetric analysis (TGA) for O_3-SWNT in argon. The temperature profile was as follows: hold for 1 h at 150 °C, ramp 5 °C/min to 600 °C, hold at 600 °C for 2.5 h.

analysis of O_3-SWNT shows a new series of IR vibrational modes, similar to that seen by Mawhinney et al. on ozonation of SWNTs deposited in a CaF_2 IR cell using 70% pure O_3.[14a] A ν(C═O) peak is observed at 1708 cm^{-1}, while another broad hydrogen-bonded peak ν(O−H) appears at 3410 cm^{-1} (not shown in Figure 4). These data suggest that carboxylic acid groups (−COOH)[12] are present on the SWNT surface. The peak at 1580 cm^{-1} is assigned to the stretching mode ν(C═C) of double bonds in the nanotube backbone near the functionalized carbon atoms[14a,15b] The relative intensity of ν(C═O)/ν(C═C) increases with reaction time in the 1−3 h regime and then tends to a stable value. This suggests that the degree of oxidation is controlled by the surface active sites and is in agreement with the change in the ω_d/ω_t Raman ratio. Ozonation is thought to proceed quickly at the end caps and kinks in SWNT, followed by reaction of the rim sites that remain.[14a] Formation of holes in the walls of the SWNT is not thought to be energetically favorable; however, the intense UV radiation combined with O_3 in our method may lead to more robust conditions.

It is noted that a 1630 cm^{-1} peak appears in the initial oxidation, which is assigned to the stretching mode ν(C═O) of quinone groups.[14] The origin of the bands at 1420 and 1370 cm^{-1} is not clear. The peaks at 1215 and 1055 cm^{-1} are attributed to the vibrational mode ν(O−C−O) of ester or ν(C−O) of carboxylic acid. Finally, we find no evidence for the formation of epoxide groups (1250 and 950−815 cm^{-1}).

Figure 5 shows a TGA analysis for O_3-SWNT. The initial weight loss is due to degassing and the evaporation of residual DMF solvent. The subsequent weight loss of ca. 20% reveals the decomposition of the oxygenated groups on nanotubes. If we assume that all the loss was due to evolution of CO_2, then we can calculate that approximately 5% of the O_3-SWNT carbons were functionalized (C is 27% of CO_2; 27% × 20% ≅ 5%). No further weight loss is observed after 5 h of heating at 600−800 °C. The spectroscopic characteristics (Figures 1b, 2c, and 4f) of the annealed sample indicate that O_3-SWNT is restored to P-SWNT after TGA.[5a,14a]

Figure 6 shows tapping-mode AFM images of O_3-SWNT and P-SWNT spin-coated on mica. The O_3-SWNT displays a series of shortened individual nanotubes, i.e., 100−800 nm in length and 0.6−1.8 nm in height. In contrast, P-SWNT shows a tangled structure of fiber

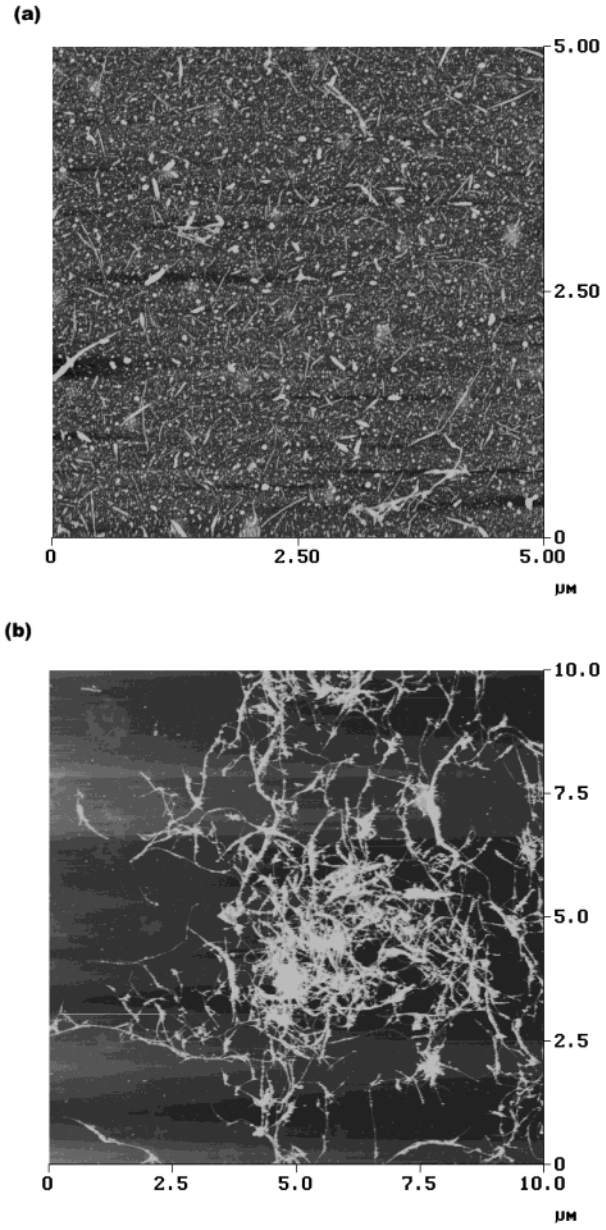

Figure 6. AFM images of (a) O_3-SWNT and (b) P-SWNT spin-coated on mica.

bundles with lengths of several microns and heights of 2−25 nm. As previously discribed,[14a] the reaction of O_3 can occur at dangling carbon bonds of the ends and wall defect sites on SWNTs, resulting in oxidation and shortening of the SWNT. The surface functional groups also destroy the extended conjugated structure of the SWNTs, resulting in decreased van der Waals forces and inducing separation of the nanotube bundles into individual SWNTs.

The surface-bound groups distort the extended π-conjugated system on nanotubes, resulting in an increase in the surface electrical resistance of O_3-SWNT. The resistance of P-SWNT is on the level of 10 Ω (two-point probe, 10 mm separation between contacts). The resistance of O_3-SWNT is increased to 200 Ω to 20 kΩ, depending on the degree of oxidation. The resistance of O_3-SWNT is thus 20−2000 times higher than that of P-SWNT.

Surface derivatization also changes the solubility[6,25,26] of the carbon nanotubes. Table 1 summarizes the solubility of O_3-SWNT and P-SWNT in the different solvents. The best solvents for SWNTs are dimethylformamide and 1,2-dichlorobenzene.[27] O_3-SWNTs show some solubility in water, while P-SWNTs are completely insoluble in water. O_3-SWNTs also exhibit an enhanced solubility in aqueous ethanolic solvent, forming a uniform and transparent solution after sonication for 5 h. This enhanced solubility could be useful for aqueous-based assembly.

Table 1. Solubility of O_3-SWNT and P-SWNT in the Different Solvents

solvent	O_3-SWNT (mg/L)[a]	PSWNT (mg/L)
dimethylformamide	113	125
1,2-dichlorobenzene	66	101
water	44	0.4
chloroform	5.5	13
ethanol	5.1	0.8
tetrahydrofuran	0.9	4.8
2-propanol	0.8	0.4

[a] The solubility was determined by UV−vis spectroscopy using a calibrated curve.[26]

Thiolacetyl-terminated oligo(phenylene ethynylene)s can be deprotected in-situ by base- or acid-promoted protocols to release the free thiol for chemical assembly on a Au surface (Scheme 1).[23] The variety of terminal functional groups in the tested oligomers provides different functionalized surfaces and alters the surface potential of the resulting SAMs. The amino group of compound **1** gives SAM-**1**, a positively charged surface, whereas the carboxylic group of compound **2** gives SAM-**2**, a negatively charged surface under the conditions of the experiments. Compound **3** bears two active thiol sites upon deprotection and can form a multilayer structure by disulfide formation if allowed a long incubation time with traces of oxygen. Therefore, assembly time for SAM-**3** was shortened.

O_3-SWNTs were chemically bound to amino-terminated SAM-**1** by an amide-forming condensation reaction, which is well-known in the synthesis of polypeptides. Figure 7 shows AFM images of O_3-SWNT/SAM-**1** assembled in DMF and H_2O solution (pH 5) for 18 h. In both cases, O_3-SWNT exhibits a high degree of coverage parallel to the surface. The carboxylic acid groups of O_3-SWNT are activated by DCC in DMF solution (or EDC in H_2O solution); further reaction with amines results in the formation of amide bonds. Furthermore, there is a Coulombic attraction between positively charged $-NH_2$ groups and negatively charged O_3-SWNTs in weak-acid solution, and the interaction of the nanotubes with $-NH_2$ groups on the surface is quite strong.[18a,b] The condensation reaction and electrostatic force lead to a stable and high-density adsorption of O_3-SWNTs on SAM-**1**.

Metal-assisted layer-by-layer (LBL) deposition[17,28] was used to form well-defined multilayer assemblies by alternate adsorption. Figure 8 shows AFM images of O_3-

(25) Niyogi, S.; Hu, H.; Hamon, M. A.; Bhowmik, P.; Zhao, B.; Rozenzhak, S. M.; Chen, J.; Itkis, M. E.; Meier, M. S.; Haddon, R. C. *J. Am. Chem. Soc.* **2001**, *123*, 733.
(26) Bahr, J. L.; Mickelson, E. T.; Bronikowski, M. J.; Smalley, R. E.; Tour, J. M. *Chem. Commun.* **2001**, 193.
(27) Ausman, K. D.; Pinter, R.; Lourie, O.; Ruoff, R. S.; Korobov, M.; *J. Phys. Chem. B* **2000**, *104*, 8911.
(28) (a) Lee, H.; Kepley, L. J.; Hong, H.-G.; Mallouk, T. E. *J. Am. Chem. Soc.* **1988**, *110*, 618. (b) Ansell, M. A.; Zeppenfeld, A. C.; Yoshimoto, K.; Cogan, E. B.; Page, C. J. *Chem. Mater.* **1996**, *8*, 591.

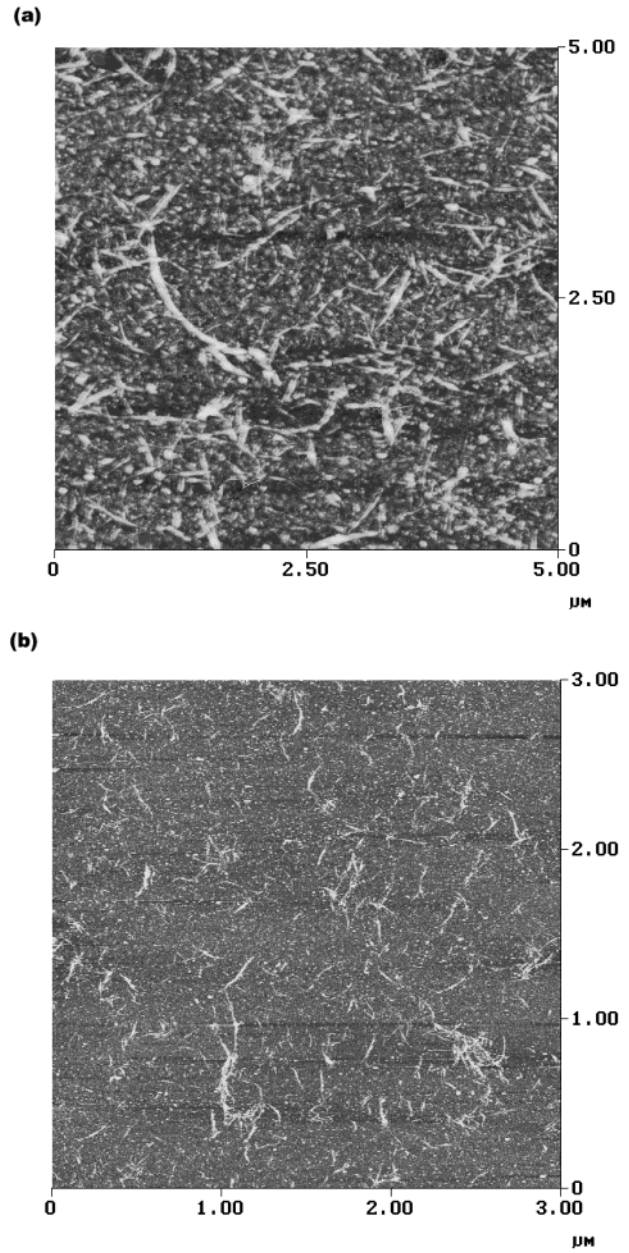

Figure 7. AFM images of O_3-SWNT/SAM-**1** assembled in (a) DMF and (b) H_2O solution (pH 5) for 18 h.

SWNT/Fe^{3+}/SAM-**2** and O_3-SWNT/Cu^{2+}/SAM-**3** assembled in DMF solution (pH 8.5) for 20 h. At the initial 1 h, most of the nanotubes are observed to randomly adsorb on the surface; as the incubation time increases (e.g. 20 h), some island structures are formed in O_3-SWNT/Fe^{3+}/SAM-**2** with widths of 35−55 nm and heights of 30−45 nm (Figure 8a). These are believed to be vertical stacking patterns of shortened O_3-SWNTs. The carboxylic groups at the ends of O_3-SWNT coordinate to the Fe^{3+} ions on the modified SAM-**2** surface, supplying an initial nucleation core, then the islands grow up through strong hydrophobic attractive interactions between the walls of the O_3-SWNTs. The surface-bound Fe^{3+} ions are in their hydroxylic forms in weak-basic solution. The increased pH provides a driving force for acid−base neutralization with carboxylic O_3-SWNT. Moreover, the chelation effect and electrostatic interac-

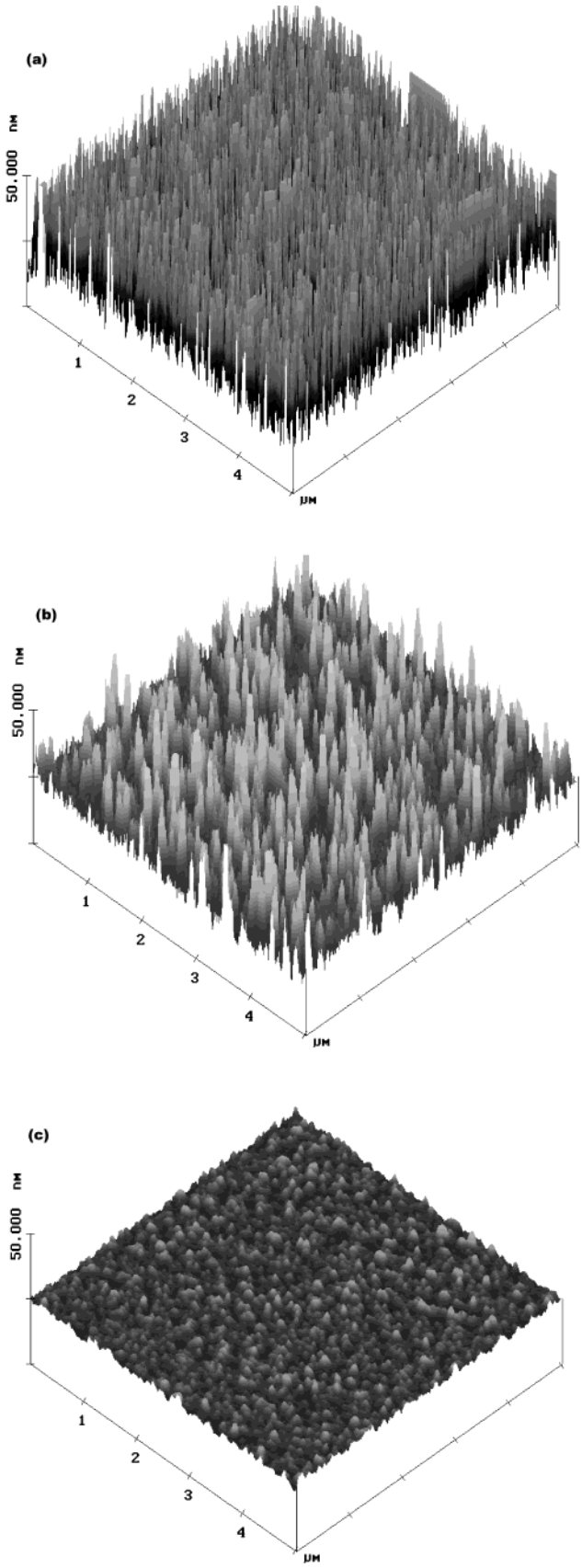

Figure 8. AFM images of (a) O_3-SWNT/Fe^{3+}/SAM-**2** assembled in DMF solution (pH 8.5) for 20 h, (b) O_3-SWNT/Cu^{2+}/SAM-**3** assembled in DMF (pH 8.5) for 20 h, and (c) Cu^{2+}/SAM-**3**.

(29) (a) Evans, D. S.; Ulman, A.; Goppert-Berarducci, K. E.; Gerenser, L. J. *J. Am. Chem. Soc.* **1991**, *113*, 5866. (b) Freeman, T. L.; Evans, S. D.; Ulman, A. *Thin Solid Films* **1994**, 784. (c) Brust, M.; Blass, P. M.; Bard, A. J. *Langmuir* **1997**, *13*, 5602.

tions facilitate the assembly. In the case of O_3-SWNT/Cu^{2+}/SAM-**3** assembly in DMF, the island structures are 70−120 nm in width and 20−45 nm in height (Figure 8b), the island size is larger, and the coverage density is lower than those of O_3-SWNT/Fe^{3+}/SAM-**2**. It is clear that the surfaces of O_3-SWNT/Cu^{2+}/SAM-**3** and O_3-SWNT/Fe^{3+}/SAM-**2** have a completely different appearance than that of the bare SAM (Figure 8c), indicating that the adsorption of carbon nanotubes forms a structure perpendicular to the gold surface. Similar results are observed for assemblies in H_2O. Multilayer structure assemblies can be obtained by LBL growth via subsequent alternate adsorption, which gives higher density coverage of SWNT.

While the increased resistance may indicate that the O_3-SWNT tubes themselves are not the best candidates for molecular wires or switches, one could envision devices wherein layers of the O_3-SWNT are used to protect molecular wires or switches in underlying SAMs from the effects of hot metal atoms being deposited as a top contact. Such a protective layer might prevent leakage of the deposited metal through to a SAM of active molecules underneath, an occurrence that can cause shorting of the device. Moreover, the combination of the O_3-SWNT and the metal may still be conductive enough for satisfactory device performance.

Conclusion

Ozonation of SWNTs induces a series of surface-bound oxygenated groups, e.g., carboxyl, ester, and quinone, resulting in improved solubility in water and an increased electrical resistance. Annealing of ozone-treated SWNTs can restore the pristine state of SWNTs. Depending on the different functionalized SAMs with thiolacetyl-terminated oligo(phenylene ethynylene)s, the carboxylic O_3-SWNTs are immobilized on the surface of rigid molecule SAMs via condensation reactions or metal-assisted LBL growth. The high coverage of O_3-SWNT may decrease the leakage current of molecular electronics devices and enhance the high charge transport between the top-layer metal and the molecular wires of assembled molecular electronics devices, a study which is currently under investigation.

Acknowledgment. This work was supported by the Defense Advanced Research Projects Agency (DARPA), the Office of Naval Research (ONR), the National Science Foundation (NSF, NSR-DMR-0073046), and NASA (NASA-JSC-NCC 9-77, OSR 99091801).

CM020273O